NACA RM E54L27

NACA

RESEARCH MEMORANDUM

PERFORMANCE OF A DOUBLE-CONE INLET WITH AND WITHOUT A SHROUD AT BELOW-DESIGN MACH NUMBERS

By Donald Pennington, Leonard Rabb, and Scott H. Simpkinson

Lewis Flight Propulsion Laboratory
Cleveland, Ohio

NATIONAL ADVISORY COMMITTEE
FOR AERONAUTICS
WASHINGTON

March 3, 1955
Declassified February 10, 1959

NATIONAL ADVISORY COMMITTEE FOR AERONAUTICS

RESEARCH MEMORANDUM

PERFORMANCE OF A DOUBLE-CONE INLET WITH AND WITHOUT A SHROUD AT BELOW-DESIGN MACH NUMBERS

By Donald Pennington, Leonard Rabb, and Scott H. Simpkinson

SUMMARY

Values of zero angle-of-attack performance of a double-cone inlet with a shroud and without the shroud have been compared through a range of mass-flow ratios at Mach numbers of 0.64, 1.50, 1.70, 1.89, and 1.98.

For a hypothetical ram-jet engine, maximum propulsive thrust was computed to be higher with the shrouded inlet at all supersonic Mach numbers tested. The inherently high additive drag associated with air spillage for the unshrouded inlet operating below its design Mach number of 2.4 accounted for the superiority of the shrouded inlet.

Presence of a long antenna probe, which protruded forward of the inlet station, seriously reduced the performance of the shrouded-inlet configuration and caused structural damage to the inlet.

INTRODUCTION

The performance of inlets with external compression is generally penalized during operation below their design Mach numbers by extremely high additive drags. A method of avoiding or reducing this penalty is desirable for ram-jet engines required to propel themselves through the transonic speed range and up to design speed. One proposed scheme involves addition of a conical extension or shroud to the basic inlet, forming in effect, a two-stage configuration. Addition of the shroud transforms the original inlet into a simple open-nose normal-shock inlet, and permits better engine performance at transonic and low supersonic Mach numbers. The shroud is designed to be discarded at the flight Mach number above which performance of the original inlet is superior to that of the simple open nose two-stage inlet.

An investigation was undertaken in the Lewis 8- by 6-foot supersonic wind tunnel to determine the effectiveness of shrouding a double-

cone inlet designed for a flight Mach number of 2.4. An inlet of the same design had previously been used on a 16-inch ram-jet missile (ref. 1). The inlet, in both the original and the shrouded configurations, was evaluated at zero angle of attack at stream Mach numbers of 0.64, 1.50, 1.70, 1.89, and 1.98. The effect on performance of the shrouded configuration of an antenna probe extending from the centerbody was also evaluated. Reynolds number per foot varied from 4.00 to 5.4×10^6.

SYMBOLS

The following symbols are used in this report:

A	area, sq ft
A_0	free-stream tube area, sq ft
A_{max}	area on which all coefficients are based (area of $16\frac{1}{8}$-in.-diam circle)(1.418 sq ft)
C_D	total external pressure drag coefficient, $(C_{d_a} + C_{d_c})$
C_d	drag coefficient, $D/q_0 A_{max}$
$C_T - C_D$	propulsive-thrust coefficient
D	drag force, lb
D_T	total external pressure drag force, lb
F_n	net internal thrust
f/a	fuel-air ratio
M	Mach number
m/m_0	mass-flow ratio, ratio of actual mass flow through the engine to mass flow through a free-stream tube equal in diameter to the cowl lip
P	total pressure, lb/sq ft abs
p	static pressure, lb/sq ft abs
q_0	stream dynamic pressure, $\frac{\gamma}{2} p_0 M_0^2$, lb/sq ft
W_f	fuel flow, lb/hr

γ ratio of specific heats

τ gas total-temperature ratio across the combustion chamber

Subscripts:

a additive

c cowl

0 free-stream station

1 engine-inlet station, cowl lip or shroud lip

2 station 4.52 in. downstream of lip of primary cowl

3 diffuser exit, combustion-chamber-inlet station, area at this station is based on a 16-in.-diameter cross section

4 160 in. from cone apex

5 nozzle-exit station

APPARATUS AND PROCEDURE

A schematic diagram of the inlet configurations investigated is shown in figure 1. The unshrouded inlet (configuration 3), a facsimile of the inlet reported in reference 1, has a double-cone spike with cone half-angles of 22° and 35°. It was so designed that the oblique shock-waves would intercept the cowl lip at a free-stream Mach number M_0 of 2.40.

The shrouded inlet consisted of the original unshrouded configuration and a conical extension, the shroud, added to it. Flow area at the shroud inlet (0.522 sq ft) is equal to the free-stream tube area calculated for the unshrouded double-cone inlet operating subcritically at a free-stream Mach number of 1.50 and a diffuser-exit Mach number of 0.22. The shrouded inlet was tested with (configuration 1) and without (configuration 2) an antenna probe projecting ahead of the conical centerbody. Inlet coordinates are given in table I.

The inlets were cold-flow tested on an engine that was strut-mounted in the 8- by 6-foot tunnel as shown in figure 1. Inlet mass flow was varied by adjusting a tail plug, which was attached to an auxiliary strut mounted from the tunnel wall. Photographs of the inlet with and without the shroud are shown in figure 2. Turnbuckle links held the shroud in position.

To aid in evaluating additive and cowl pressure drag, the model was instrumented along the cowl and the spike with a series of wall static orifices located on the top and the bottom surfaces. Four static-pressure tubes and two slotted self-averaging-type total-pressure tubes were located at station 2 (see fig. 1). Four equally spaced wall static-pressure taps were located at station 4.

At supersonic free-stream Mach numbers, air flow through the engine was calculated from the average of the four static-pressure measurements at station 4, the calibrated area ratio between stations 4 and 5 for each plug position, and by assuming a Mach number of 1.0 at station 5. Air flow through the engine at $M_0 = 0.64$ was obtained from the pressure measurements at station 2. Total temperature within the engine was assumed to be equal to the free-stream total temperature. Diffuser-exit Mach number M_3 was obtained from the measured engine air flow and by assuming the total pressure at station 3 equal to the total pressure at station 4. For each value of M_3, a thrust coefficient for a hypothetical ram-jet engine was computed. The assumptions for these computations were: a total-pressure drop across the flame holder equal to twice the dynamic pressure at station 3, and an engine combustor and outlet of constant area.

Cowl-pressure drags were computed from an integration of static pressure along the cowl. Additive drag was computed as the difference between momentum at the inlet station and that in the free-stream. For the unshrouded configuration, pressure force on the spike (determined from an integration of the spike pressures) should also be included in the additive-drag calculation. The inlet momentum was calculated from the measured engine air flow; it was evaluated by assumption of an average inlet Mach number and a static pressure derived from the total pressure at the inlet station. Inlet-station total pressure was considered equal to the total pressure measured at station 2. Calculations of specific fuel consumption included the assumption of 100-percent combustion efficiency. The unshrouded inlet pulsed severely for some subcritical flow conditions at free-stream Mach numbers of 1.89 and 1.98.

Although the data obtained from the pressure instrumentation during pulsing may represent time-average values that are quantitatively inaccurate, the information is included for its qualitative significance.

RESULTS AND DISCUSSION

Internal Diffuser Performance

Values indicating internal performance of the shrouded and the unshrouded inlet are presented in figures 3(a) and (b), respectively. Theoretical values of normal-shock pressure recovery, indicated along the ordinate of figure 3(a), are close to the maximum recoveries observed experimentally. The open symbols of figure 3(a) are for the shrouded

inlet without the antenna probe, and the tailed symbols at $M_0 = 1.98$ represent data for the shrouded inlet with the antenna probe installed. At $M_0 = 1.98$ and $M_3 = 0.21$, total-pressure recovery for the shrouded inlet was 18 points less with the antenna probe than without the probe. This difference in total-pressure recovery is attributed to shock-boundary-layer interaction that caused flow separation along the antenna probe and resulting antenna-probe vibration. This vibration was of sufficient amplitude to damage the inlet materially, and the antenna probe was therefore removed for subsequent tests of the shrouded inlet. All following references to the shrouded inlet in this text refer to the shrouded-inlet configuration without the antenna probe. For conditions corresponding to the data presented in figure 3(a), operation of the shrouded inlet was stable over the entire range of variables.

Figure 3(b) presents the diffuser performance data for the unshrouded inlet. The severe drop in subcritical diffuser total pressure recovery at free-stream Mach numbers of 1.89 and 1.98 was coincident with excessive pulsing of the inlet. As expected, the critical total-pressure recovery of the unshrouded inlet was higher than that observed for the shrouded inlet.

Figure 3 also presents values of mass-flow variation for both configurations. Since the mass-flow ratio m/m_0 is defined as the ratio of the mass flow actually captured by the inlet to the mass flow through a free-stream tube having a diameter equal to the cowl-lip diameter, this parameter can only be used to compare the air flow of inlets having the same capture area. Capture area of the unshrouded inlet was 88 percent greater than that of the shrouded inlet; a mass-flow ratio of 1.0 for the shrouded inlet would therefore correspond to a mass-flow ratio of only 0.53 for the unshrouded inlet. To compare the air-handling ability of the two configurations, a mass-flow ratio A_0/A_{max} based on maximum engine cross-sectional area should be used. Such a comparison is made below at critical flow for $M_0 = 1.5$ and $M_0 = 2.0$.

M_0		Unshrouded inlet	Shrouded inlet
1.5	P_3/P_0	0.890	0.813
	m/m_0	.580	1.000
	A_0/A_{max}	.400	.368
2.0	P_3/P_0	0.835	0.665
	m/m_0	.763	1.000
	A_0/A_{max}	.527	.368

From internal flow considerations alone, it appears that the unshrouded inlet is superior to the shrouded inlet in the speed range

between $M_0 = 1.5$ and $M_0 = 2.0$. It not only has equivalent or better pressure recoveries, but handles a greater air flow as well.

Schlieren photographs of the unshrouded inlet at supercritical mass-flow ratios are presented in figure 4. It should be noted that the Mach numbers of the tests are all below the design value of 2.4, which accounts for the large amount of spillage indicated by the shock structure.

Figures 5(a) and (b) present the breakdown in the subcritical total pressure recovery for the shrouded and for the unshrouded configurations, respectively. The diffuser total-pressure recovery P_3/P_0 has been broken down into entrance total-pressure recovery P_2/P_0 and subsonic diffuser total-pressure recovery P_3/P_2. The subcritical entrance recovery P_2/P_0 of both configurations remained fairly constant and was approximately equal to the entrance shock losses. Since the entrance losses of the shrouded inlet are not entirely shock losses, but include some total-pressure drop due to viscous effects on the flow in the shroud from station 0 to station 2, it must be concluded that this latter loss was negligible. When excessive subcritical pulsing was encountered with the unshrouded inlet at $M_0 = 1.89$ and $M_0 = 1.98$, severe entrance losses resulted (fig. 5(b)).

The trend (and value) of the subsonic diffuser total-pressure recovery P_3/P_2 was essentially the same for both configurations. An increase in this pressure recovery was observed as velocity of the internal flow was lowered. It is this improved subsonic diffuser performance that causes over-all total-pressure recovery P_3/P_0 to rise as the inlet flow decreases to subcritical values. A slight improvement in subsonic diffuser performance P_3/P_2 as stream velocity was lowered was noted with the unshrouded inlet (fig. 5(b)). No effect was observed with the shrouded configuration (fig. 5(a)).

Drag

For a complete comparison of the shrouded and the unshrouded configurations, values of drag as well as of internal performance should be evaluated. Values of total and component pressure drag of each configuration were therefore determined at zero angle of attack. As reported herein, total drag coefficient does not include friction drag, and thus represents only the sum of the cowl-pressure drag and the additive drags.

Cowl-pressure drag. - Cowl-pressure drag coefficient $C_{d,c}$ is presented for the shrouded and the unshrouded configurations in figures 6(a) and (b), respectively. In figure 6(a), $C_{d,c}$ appears to vary linearly with m/m_0, and increases progressively with free-stream Mach number at a given m/m_0. In contrast, the cowl-drag coefficient for the unshrouded inlet (fig. 6(b)) does not appear to be either a linear function of m/m_0, or to increase progressively with M_0. Transonic

values of $C_{d,c}$ obtained in free flight (ref. 2) are also included in figure 6(b) and show fair agreement with the data at $M_0 = 0.64$.

Additive drag. - The additive drag coefficients $C_{d,a}$ are presented in figures 7(a) and (b) for the shrouded and the unshrouded configurations, respectively. For the shrouded-inlet configuration, the additive drag is the arithmetic difference between momentum of the engine air flow at the free-stream station and at the cowl-lip station. The theoretical additive drag for a normal-shock inlet operating at a Mach number of 1.8 (ref. 3) is shown on this curve; as would be expected, it falls between the test data for the shrouded inlet operating at Mach numbers of 1.70 and 1.89.

The additive drag coefficient for the unshrouded inlet (fig. 7(b)) also generally followed the theoretically anticipated trend with changes in M_0 and in m/m_0. However, pulsing flow at $M_0 = 1.89$ and $M_0 = 1.98$, which has been previously mentioned, affected the additive drag coefficient and caused a departure from the trends observed at the other free-stream Mach numbers.

A comparison of the additive drag coefficients of the shrouded and the unshrouded configurations indicates the large drag penalty associated with the inherent air spillage of the unshrouded inlet at below-design Mach numbers. For example, at a diffuser exit Mach number M_3 of 0.20, the following was observed:

	Free-stream Mach number			
	1.98		1.50	
	Shrouded inlet	Unshrouded inlet	Shrouded inlet	Unshrouded inlet
m/m_0	0.962	0.660	0.870	0.498
A_0/A_{max}	.354	.456	.320	.344
$C_{d,a}$	.02	.322	.046	.336

Total drag. - The variation of total drag coefficient C_D with mass-flow ratio is presented in figures 8(a) and (b) for the shrouded and the unshrouded configurations, respectively. The free-flight data of reference 2 is included in figure 8(b). Since the additive drag constitutes the major portion of the total drag (neglecting friction), the trends are essentially the same for the C_D curves as for the C_{d_a} curves. In the region of $M_0 = 1.5 - 2.0$, minimum drag of the unshrouded inlet is five times as great as minimum drag of the shrouded inlet.

Engine Performance

For computation of ram-jet engine performance over a range of Mach numbers from 1.5 to 2.0, a constant-area combustion chamber and exit nozzle were assumed. The assumed variations of engine total-temperature ratio τ and of gasoline fuel-air ratio f/a with change in M_3 are shown in figure 9. Computed thrust coefficient was combined with observed total-drag coefficient C_D to determine specific fuel consumption $\frac{W_f}{F_n - D_T}$ (fig. 10).

The shrouded inlet (fig. 10(a)) indicated a continuous rise in $C_T - C_D$ as M_3 is reduced. For an engine utilizing a hydrocarbon fuel, such as gasoline, the limiting diffuser-exit Mach number M_3 would be 0.16 (fig. 9). To extend the propulsive-thrust calculations, heat additions greater than those obtainable with gasoline were assumed. The curve of $C_T - C_D$ for the unshrouded inlet (fig. 10(b)) also shows a rising characteristic with decreasing M_3 until severe pulsing is encountered (at $M_0 = 1.89$ and 1.98). Propulsive-thrust coefficient was more sensitive to changes in free-stream Mach number with the unshrouded inlet than with the shrouded inlet.

Specific fuel consumption shows only slight dependence on the free-stream Mach number with the shrouded inlet. With the unshrouded inlet, however, it changes markedly with free-stream Mach number. For example, at $M_3 = 0.22$, specific fuel consumption with the unshrouded inlet decreased from 4.63 to 3.1 as free-stream Mach number increased from 1.50 to 1.98.

The shrouded and unshrouded configurations are compared in figures 11 and 12 on the basis of minimum possible specific fuel consumption and maximum possible $C_T - C_D$. The values of $C_T - C_D$ correspond to diffuser-exit Mach numbers of 0.160 with the exception of the values for $M_0 = 1.89$ and 1.98. These points correspond to values of $M_3 = 1.70$ and 0.184, respectively, and represent the maximum propulsive-thrust coefficient achievable at these two Mach numbers before encountering severe pulsing. It is obvious from figures 11 and 12 that addition of the shroud improved the performance of the unshrouded double-cone inlet, even at free-stream Mach numbers from 1.5 to 1.98. Poor performance of the unshrouded inlet at speeds below $M_0 = 1.5$ was to be expected. However, it was surprising to observe that the beneficial effects of the shroud extend to Mach numbers as high as 1.98. Maximum propulsive-thrust coefficient observed for the shrouded inlet was higher than that for the unshrouded inlet by 11 percent at $M_0 = 1.98$ and 51 percent at $M_0 = 1.50$. The shrouded inlet also showed lower (13 percent at $M_0 = 1.98$) minimum specific fuel consumption than the unshrouded inlet.

SUMMARY OF RESULTS

The zero-angle-of-attack performance of a double-cone inlet designed for a free-stream Mach number $M_0 = 2.4$ (cone half-angles of 22° and 35°) with and without a shroud has been determined in the Lewis 8- by 6-foot supersonic wind tunnel at $M_0 = 0.64$ and $M_0 = 1.5$ through 2.0. The following results were obtained:

1. Although total-pressure recovery of the unshrouded inlet was higher at all Mach numbers, minimum drag was 5 times that of the shrouded inlet because of air-flow spillage. Consequently, when the two configurations are applied to a hypothetical ram-jet engine, better performance is indicated with the shrouded configuration. The gain in maximum thrust-minus-drag coefficient for the hypothetical engine amounted to 11 percent at a Mach number of 1.98 and 51 percent at a Mach number of 1.50. Corresponding reductions in minimum specific fuel consumption were indicated.

2. The peak pressure recoveries observed for the shrouded inlet are essentially equal to the theoretical normal-shock values at corresponding free-stream Mach numbers.

3. Presence of a long antenna probe, which protruded forward of the centerbody, had a damaging effect on the performance of the shrouded-inlet configuration, reducing diffuser total-pressure recovery at $M_0 = 1.98$ by 18 points.

Lewis Flight Propulsion Laboratory
National Advisory Committee for Aeronautics
Cleveland, Ohio, December 23, 1954

REFERENCES

1. Disher, John H., Kohl, Robert C., and Jones, Merle L.: Free-Flight Performance of a Rocket-Boosted, Air-Launched 16-Inch-Diameter Ram-Jet Engine at Mach Numbers up to 2.20. NACA RM E52L02, 1953.

2. Jones, Merle L., Rabb, Leonard, and Simpkinson, Scott H.: Drag Data for 16-Inch-Diameter Ram-Jet Engine with Double-Cone Inlet in Free Flight at Mach Numbers from 0.7 to 1.8. NACA RM E54H02, 1954.

3. Sibulkin, Merwin: Theoretical and Experimental Investigation of Additive Drag. NACA RM E51B13, 1951.

TABLE I. - INLET COORDINATES

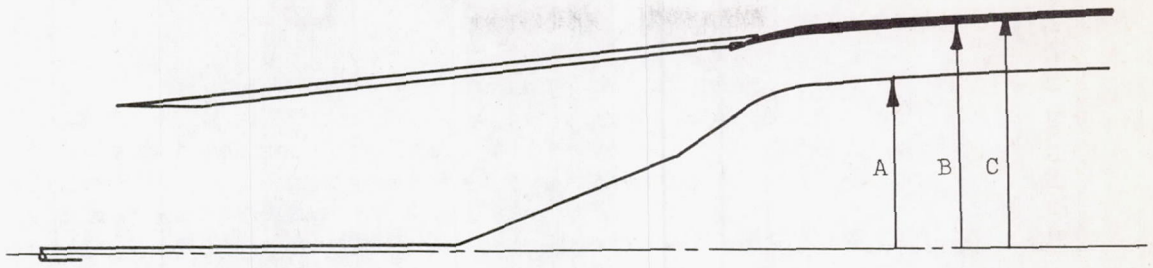

Station, in.	Location	A, in.	B, in.	C, in.	Miscellaneous
-10.8	Lip of blow-off cowl, station 1	----	4.90	---	Lip angle, 6° Capture area, 0.522 sq ft
-8			4.90	Straight taper	
0	Spike tip	0	Straight taper		22° half-angle
7.95	Beginning second cone	3.20			35° half-angle
8.65			6.70		
9.48	Lip of double cone cowl, station 1				Lip angle, $23\frac{1}{2}$° Capture area, 0.979 sq ft
			6.70		
10.42		4.90	7.00	7.20	
12		5.35	7.15	7.27	
14	Station 2	5.55	7.35	7.47	
18		5.80	7.60	7.62	
22		5.90	7.70	7.82	
28		6.05	7.90	8.02	
$36\frac{1}{4}$		6.05	8.00	8.12	
54		5.70	8.00		
64		4.50	7.45		
70		2.60	7.40	Straight taper	
74.5	End of center-body		Straight taper		
94.3	Tail-pipe entrance				
115	Station 3		8.00		
160	Station 4				
170	Converging nozzle; entrance		Straight taper		
188	Converging nozzle; exit, station 5		5.78	5.90	

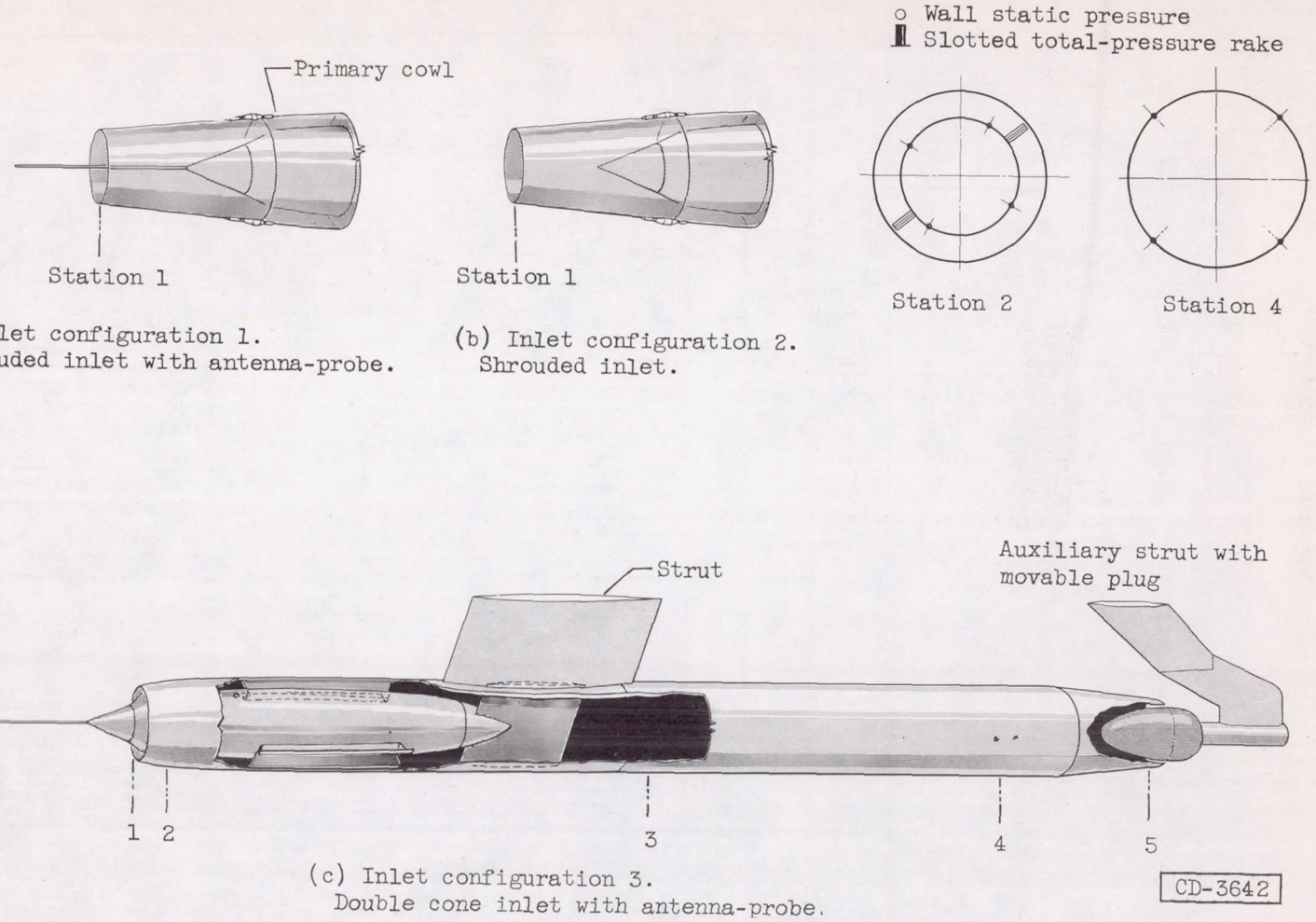

(a) Inlet configuration 1. Shrouded inlet with antenna-probe.

(b) Inlet configuration 2. Shrouded inlet.

(c) Inlet configuration 3. Double cone inlet with antenna-probe.

Figure 1. - Schematic diagram of 16-inch ram-jet engine with inlet configurations tested.

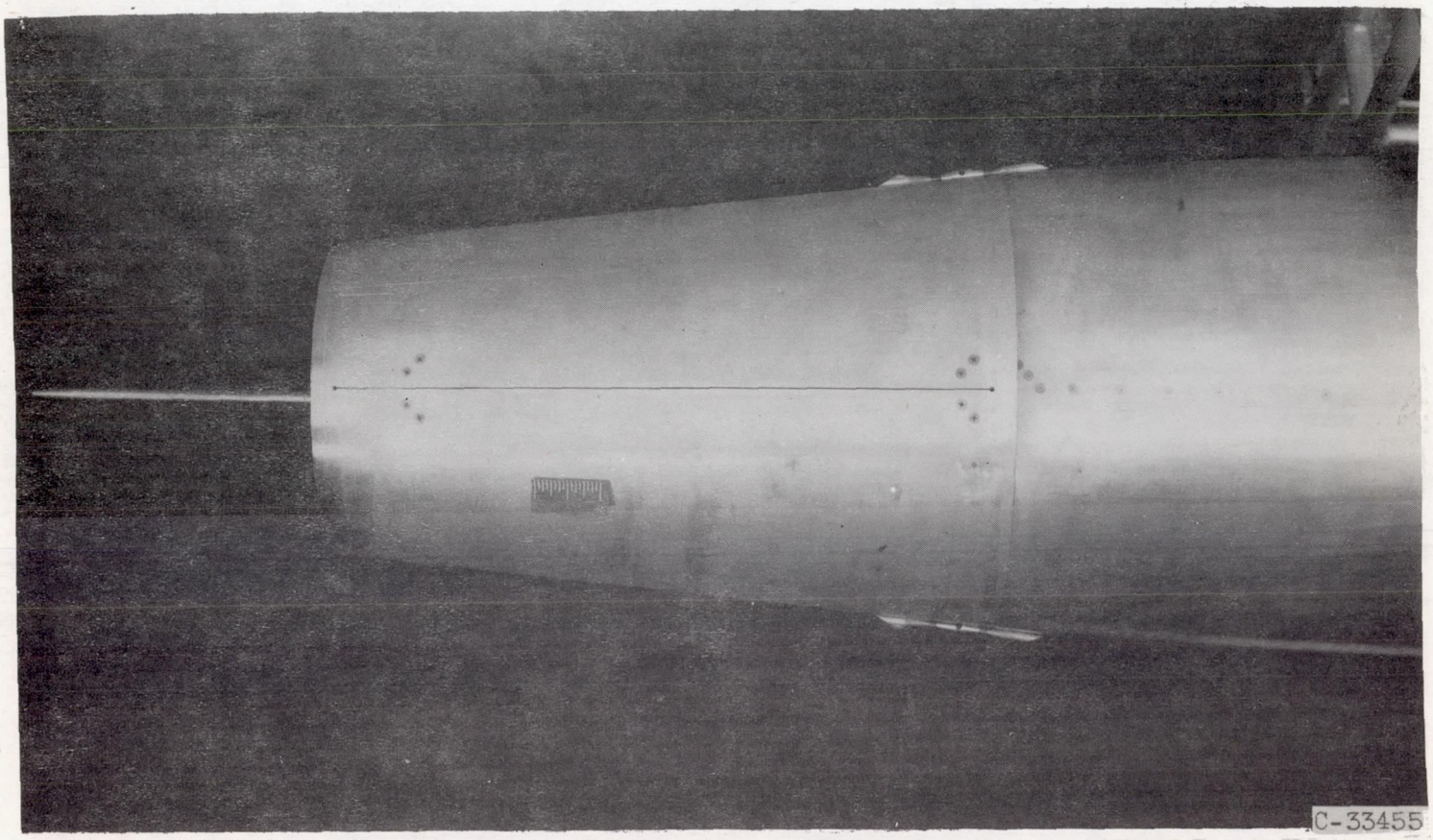

(a) Shrouded inlet.

Figure 2. - Inlet configurations with antenna probe protruding forward of inlet station.

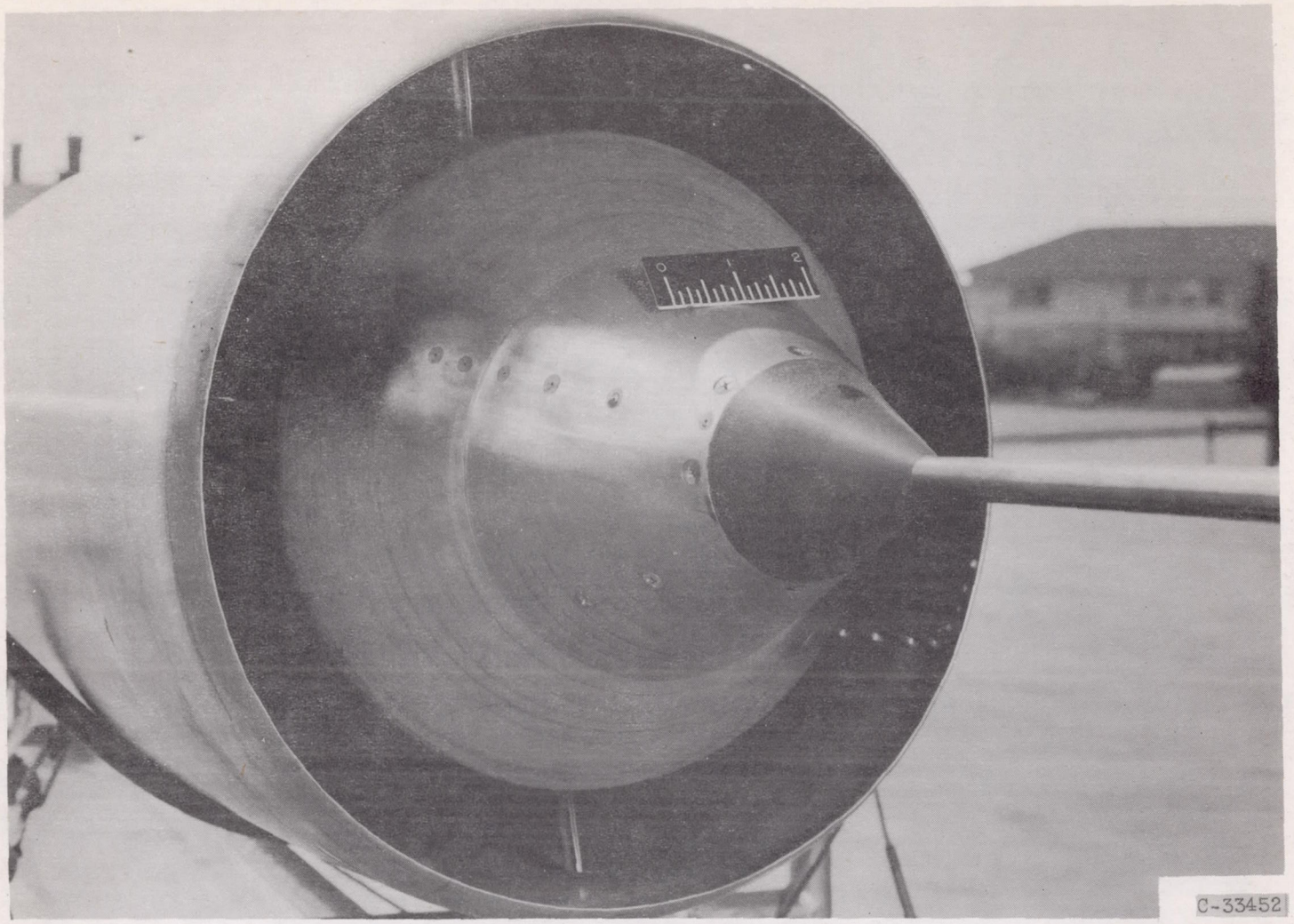

(b) Unshrouded double-cone inlet.

Figure 2. - Concluded. Inlet configurations with antenna probe protruding forward of inlet station.

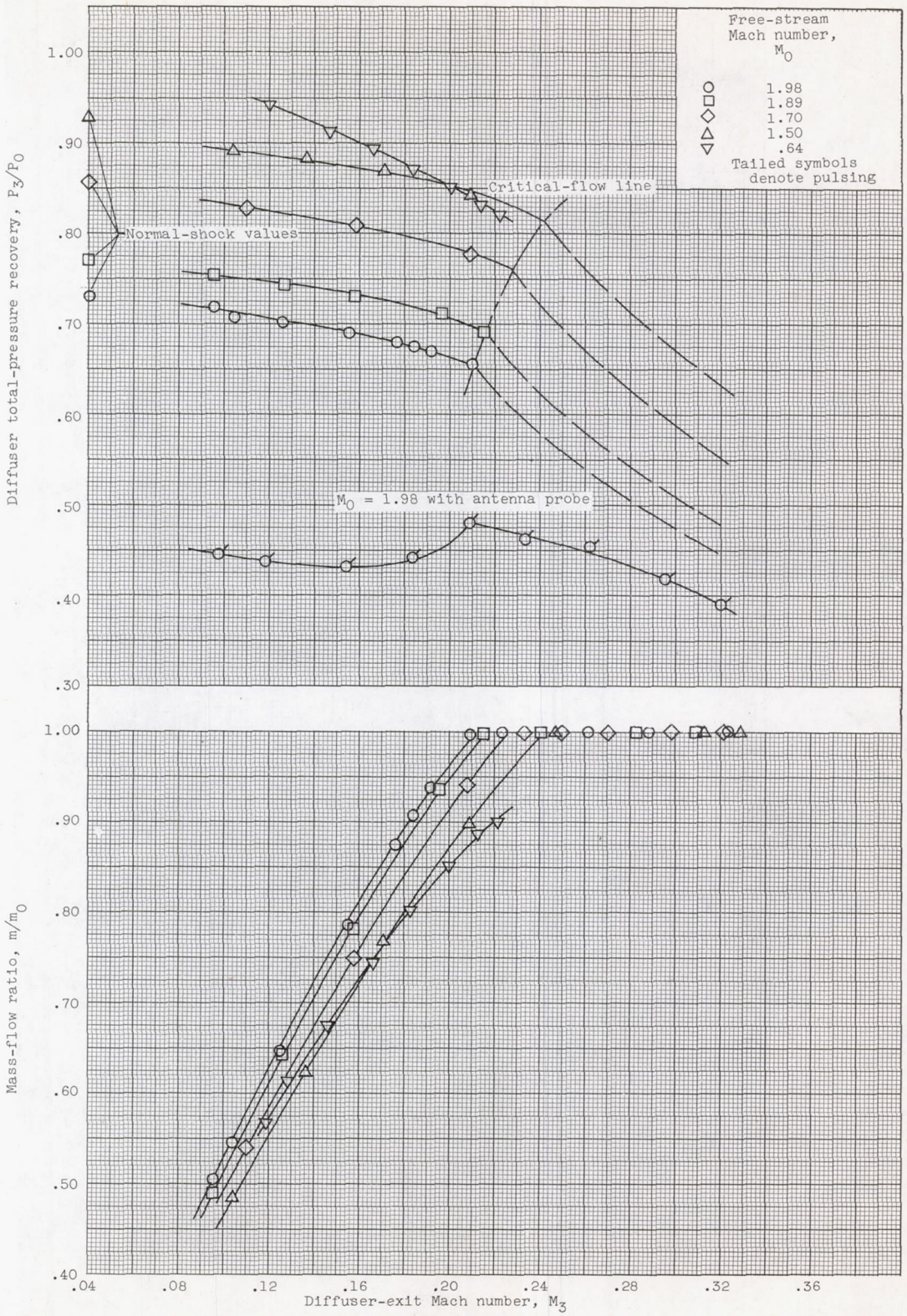

(a) Shrouded inlet.

Figure 3. - Total-pressure recovery and mass-flow characteristics at zero angle of attack.

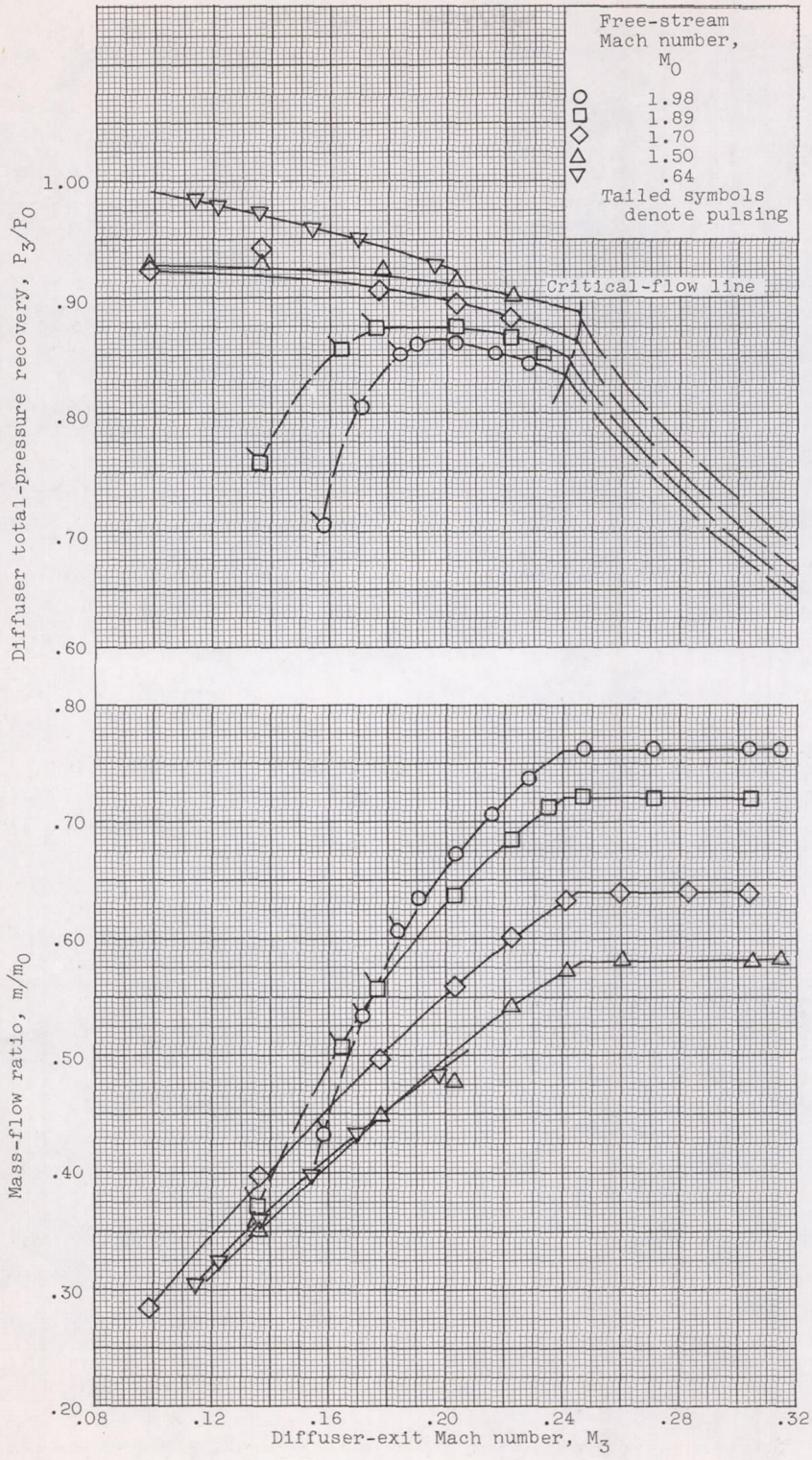

(b) Unshrouded inlet.

Figure 3. - Concluded. Total-pressure recovery and mass-flow characteristics at zero angle of attack.

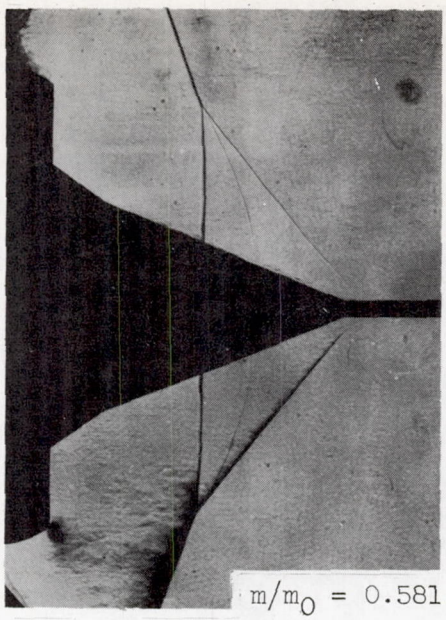

M_0 = 1.50

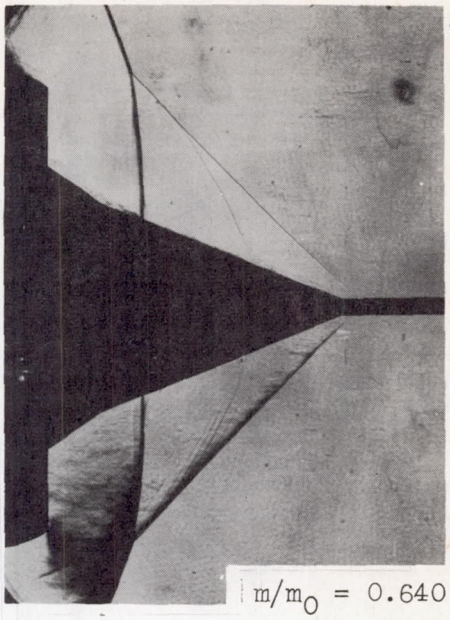

M_0 = 1.70

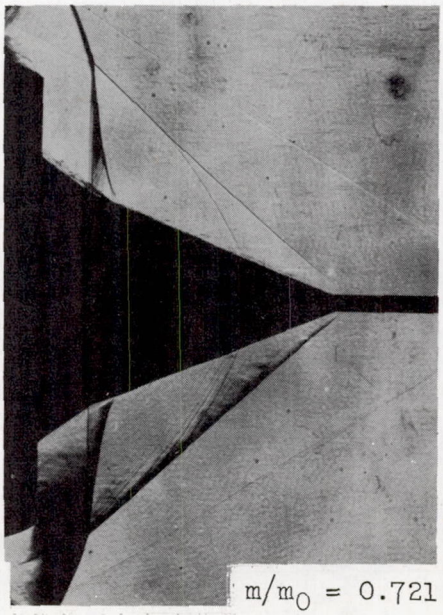

M_0 = 1.89

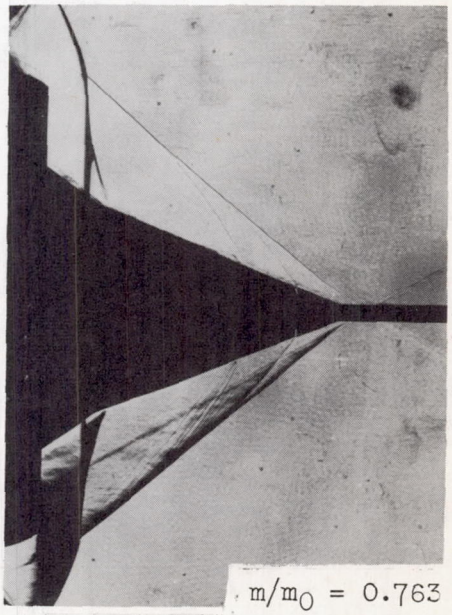

C-37283

M_0 = 1.98

Figure 4. - Schlieren photographs of the unshrouded double-cone inlet operating supercritically at below-design Mach numbers.

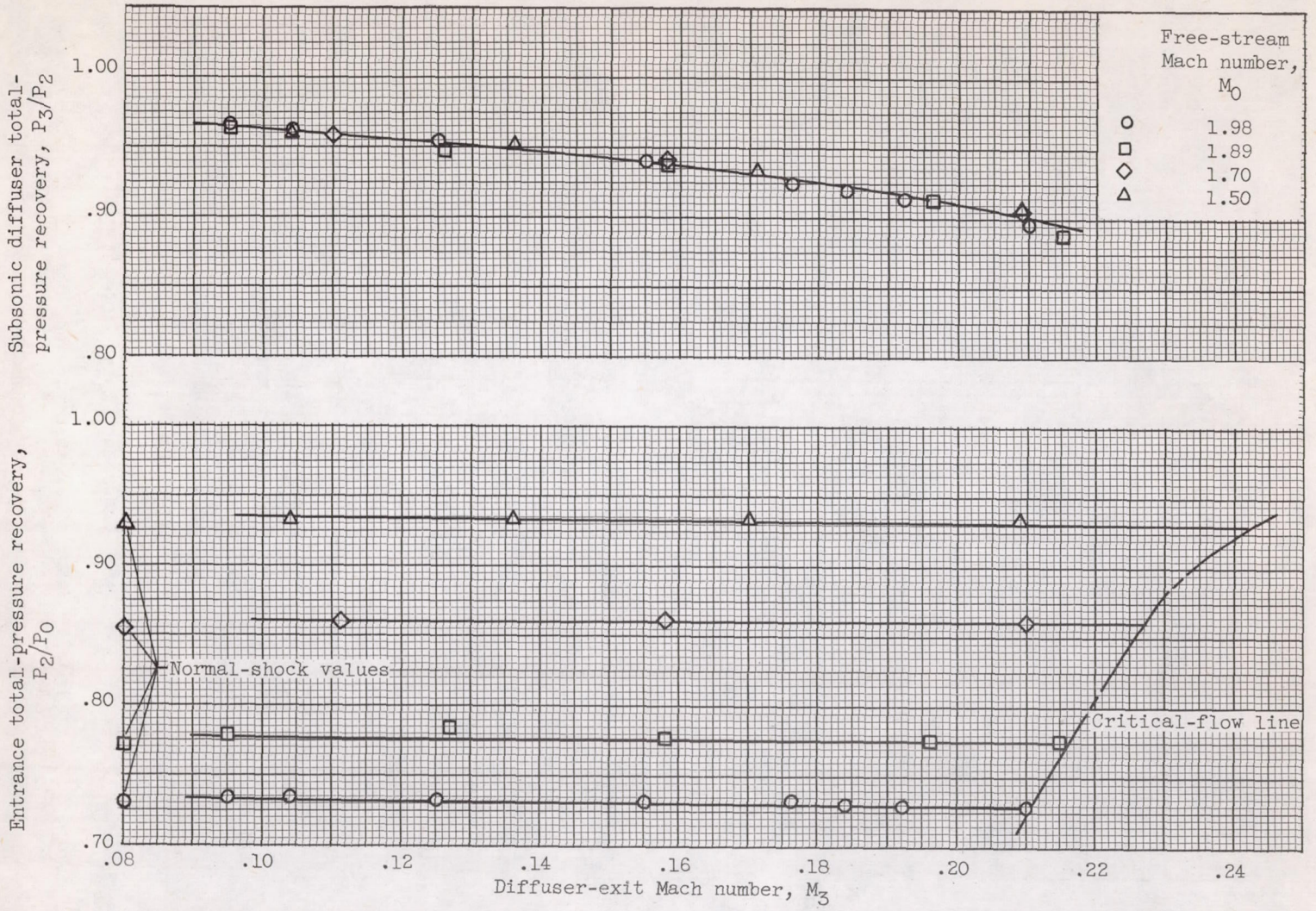

(a) Shrouded inlet.

Figure 5. - Subcritical entrance and subsonic diffuser total-pressure recovery.

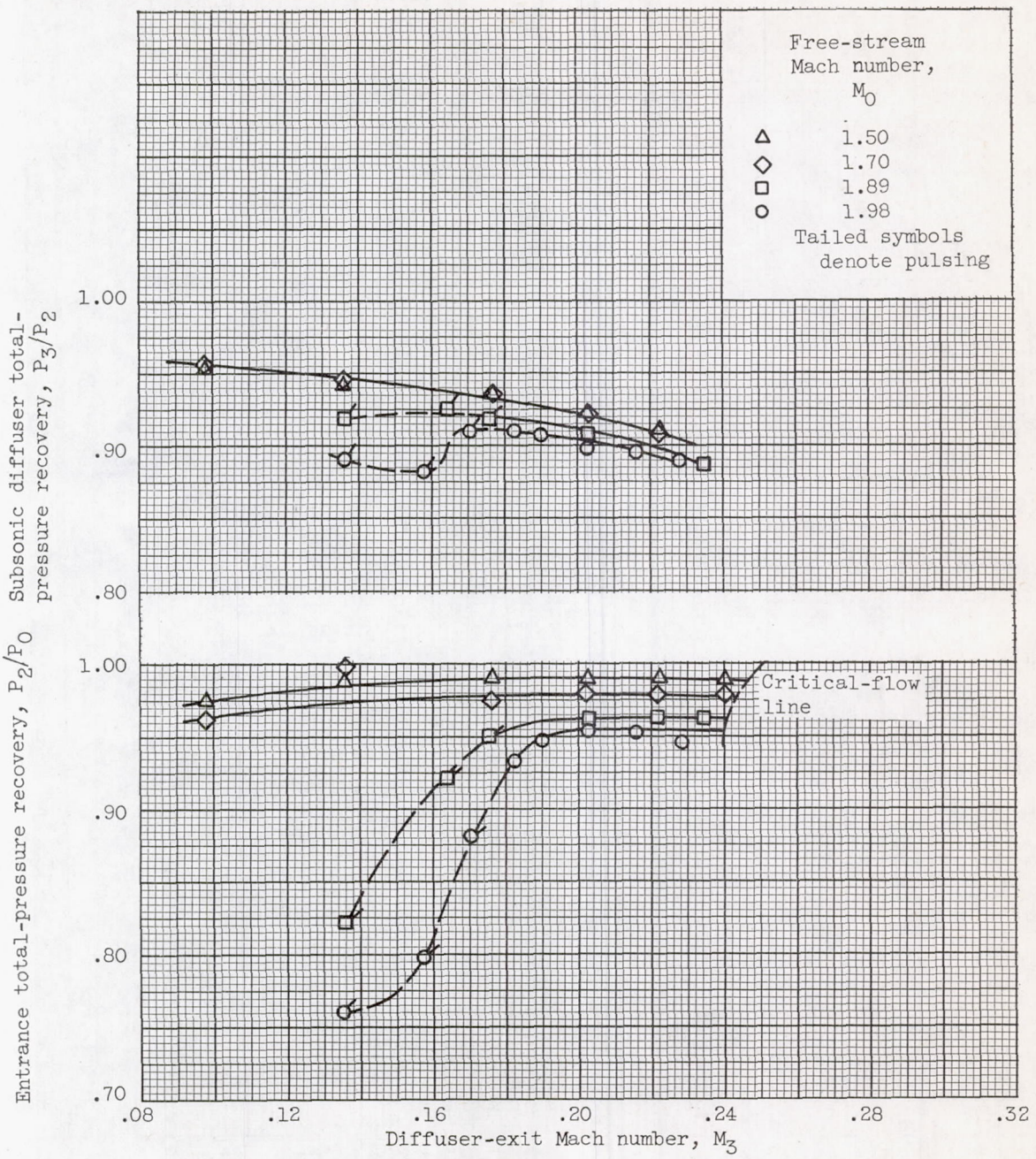

(b) Unshrouded inlet.

Figure 5. - Concluded. Subcritical entrance and subsonic diffuser total-pressure recovery.

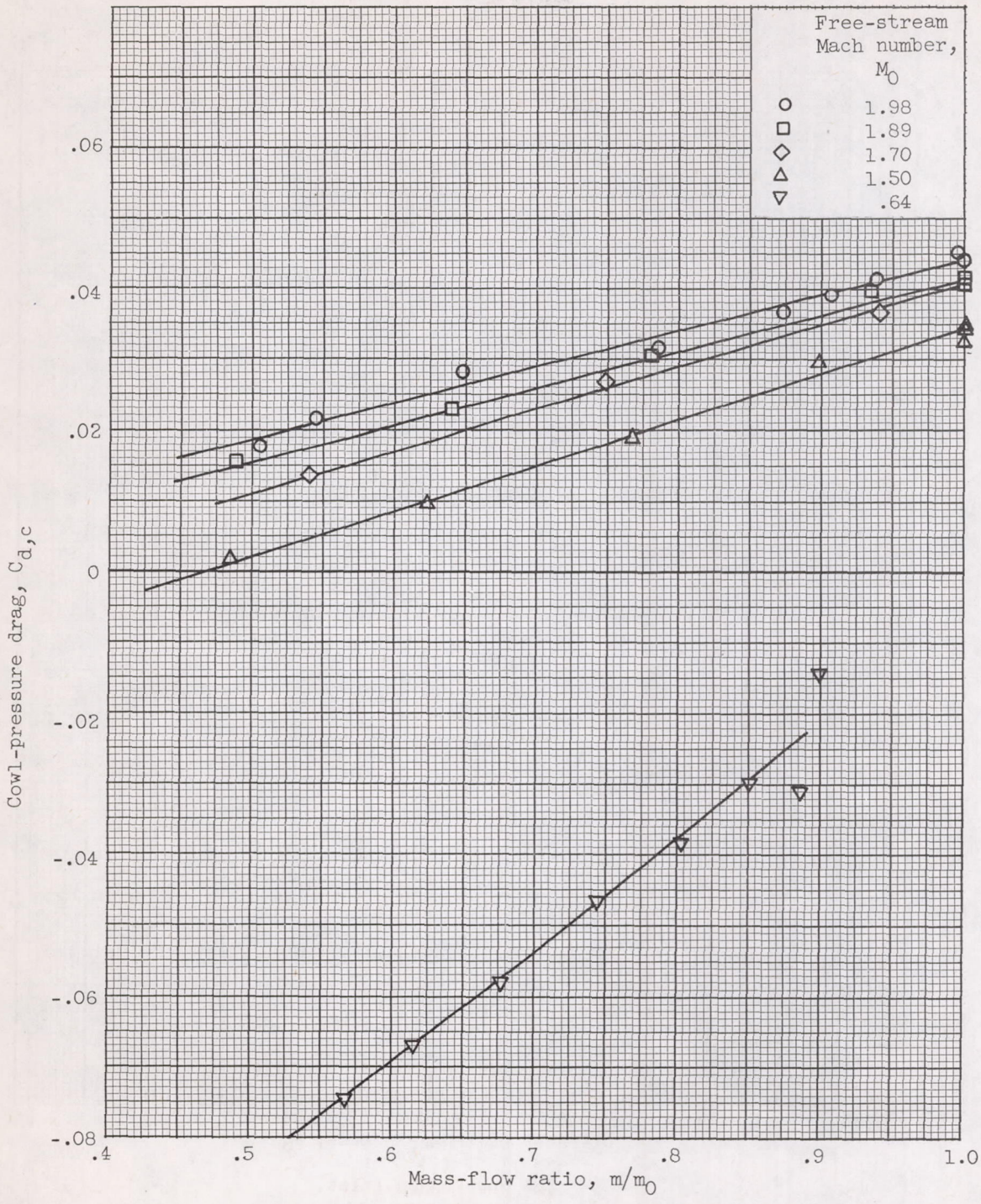

(a) Shrouded inlet.

Figure 6. - Variation in cowl-pressure drag coefficient with mass-flow ratio.

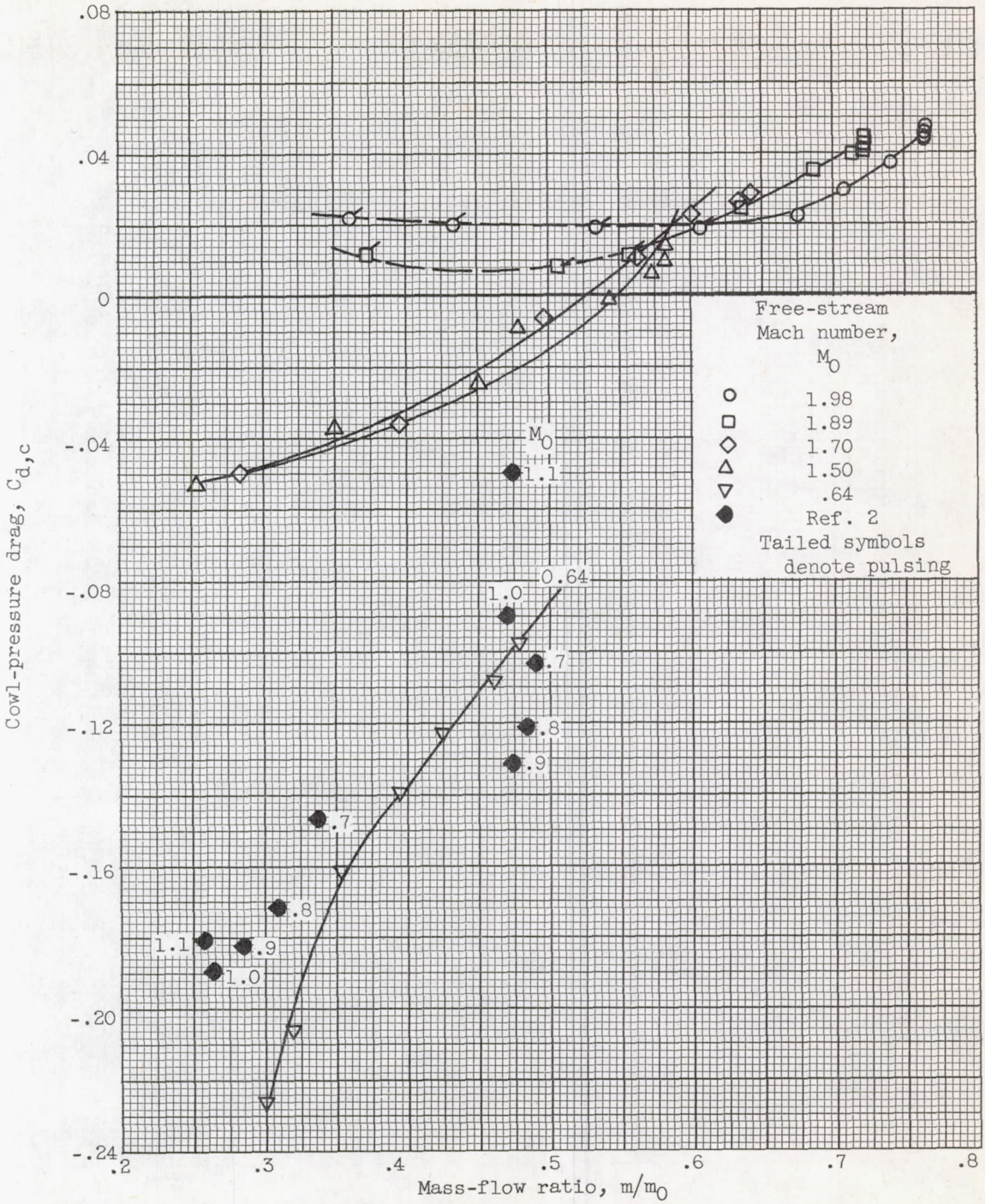

(b) Unshrouded inlet.

Figure 6. - Concluded. Variation in cowl-pressure drag coefficient with mass-flow ratio.

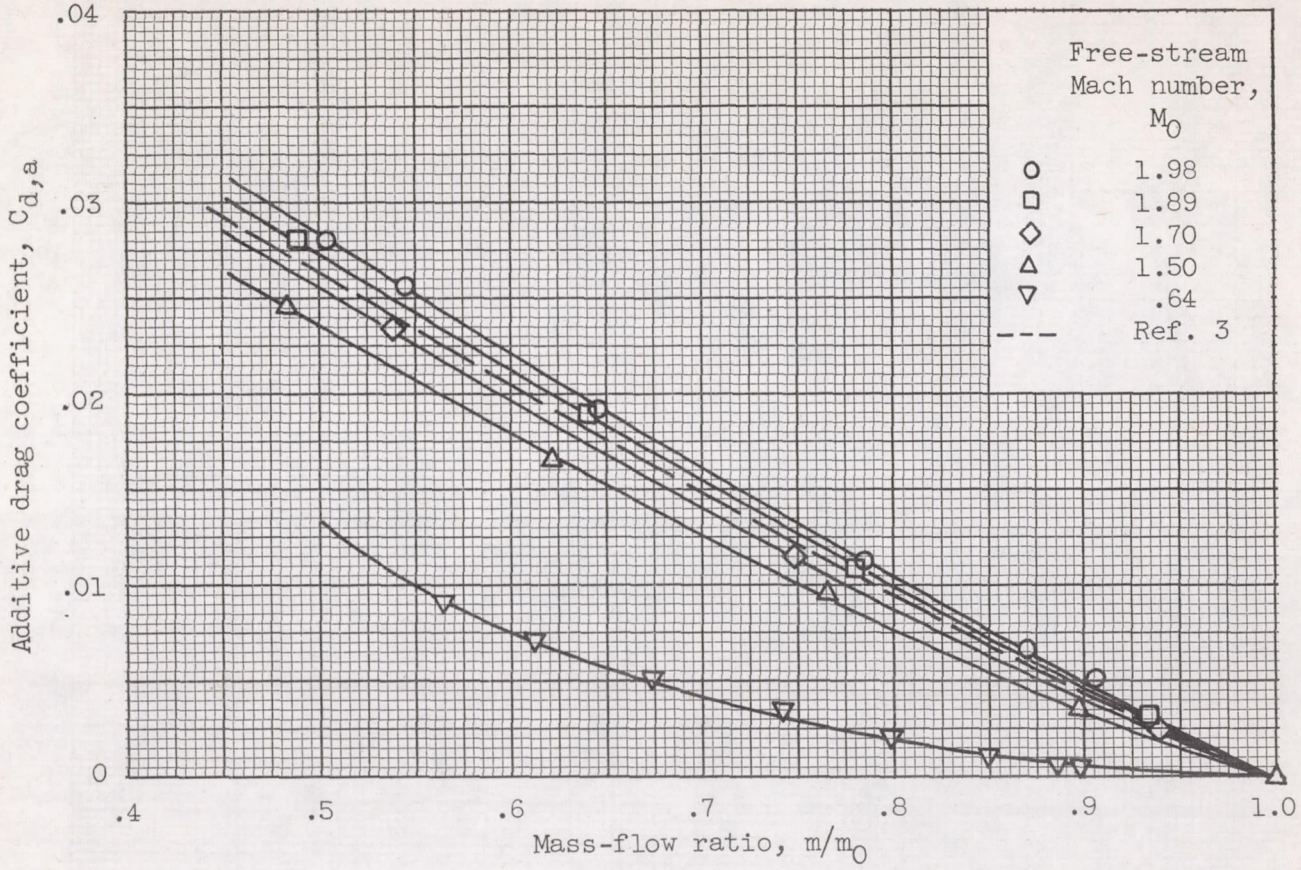

(a) Shrouded inlet.

Figure 7. - Variation in additive drag coefficient with mass-flow ratio.

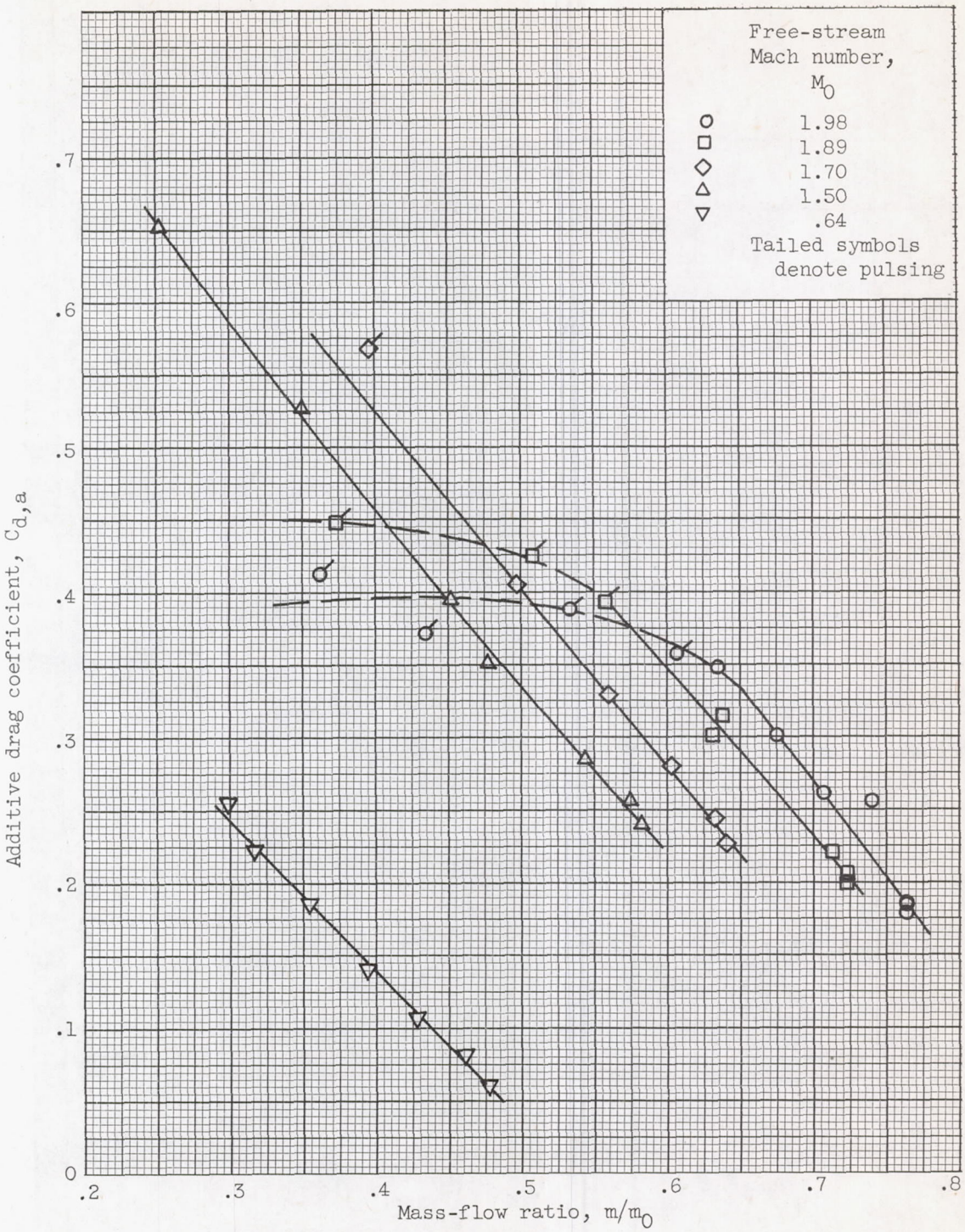

(b) Unshrouded inlet.

Figure 7. - Concluded. Variation in additive drag coefficient with mass-flow ratio.

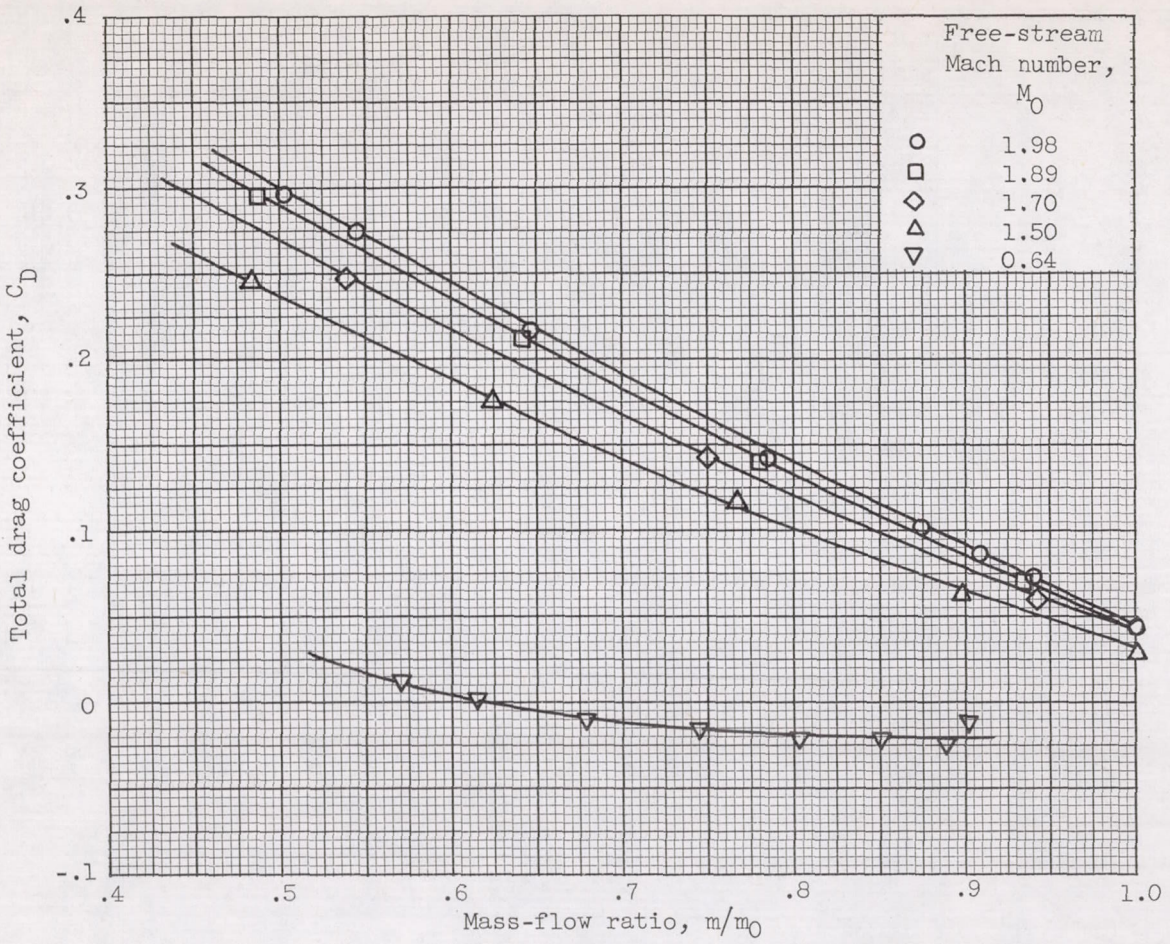

(a) Shrouded inlet.

Figure 8. - Variation in sum of additive and cowl-pressure drags with mass-flow ratio.

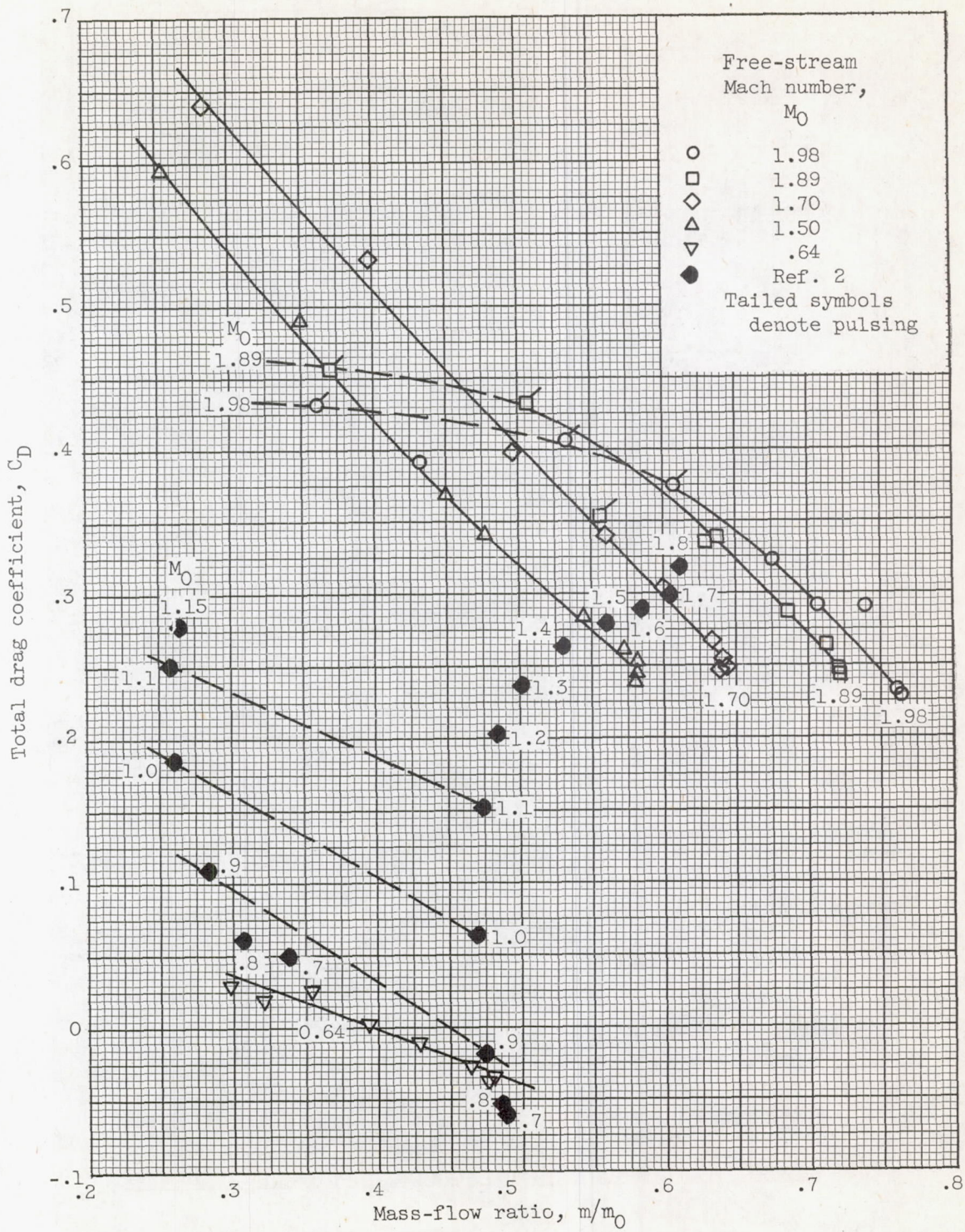

(b) Unshrouded inlet.

Figure 8. - Concluded. Variation in sum of additive and cowl-pressure drags with mass-flow ratio.

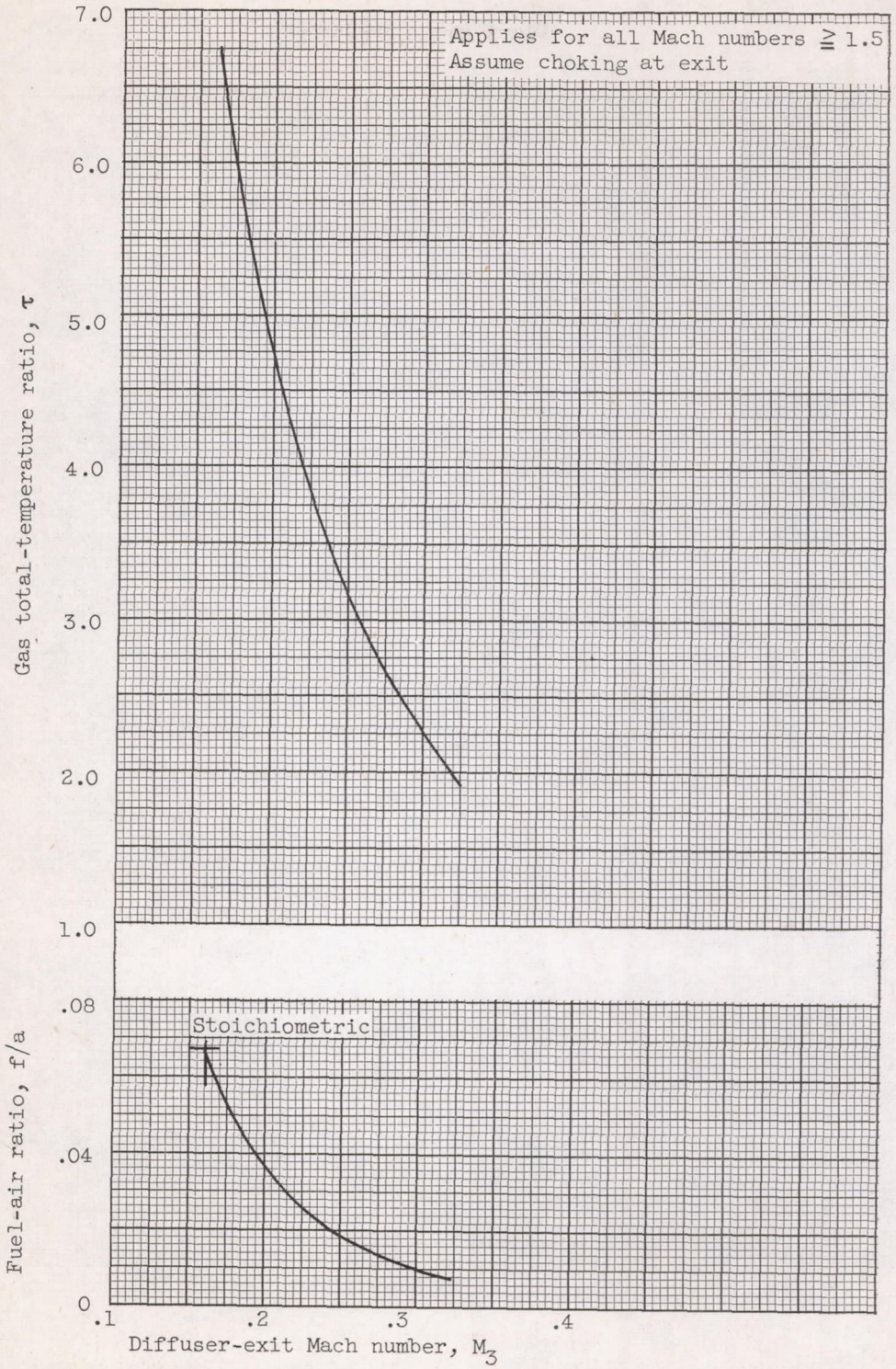

Figure 9. - Assumed combustion-chamber performance. Values used for values of free-stream Mach number above 1.5; choking at nozzle exit and 100 percent combustion efficiency assumed.

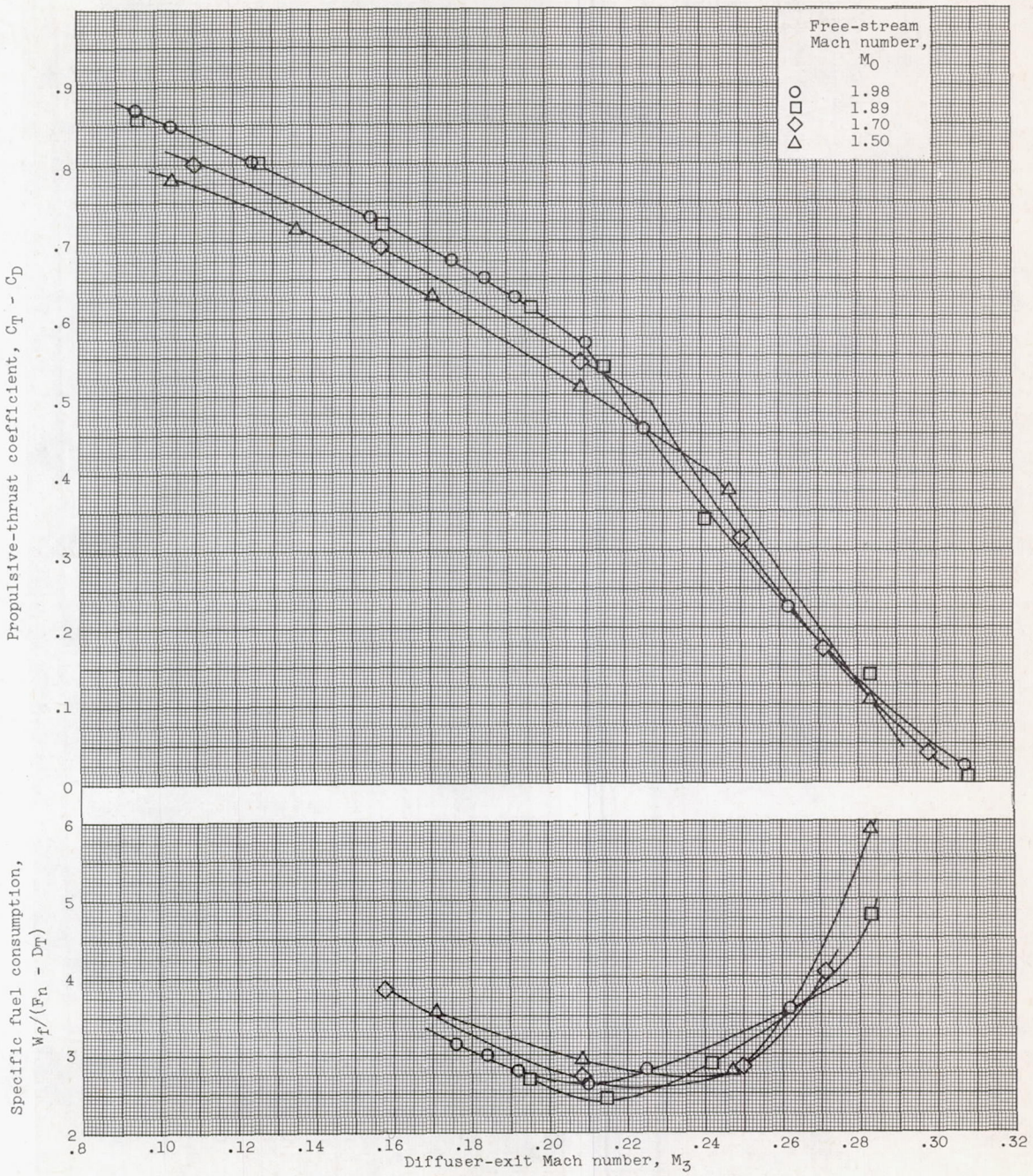

(a) Shrouded inlet.

Figure 10. - Propulsive thrust coefficient and specific fuel consumption.

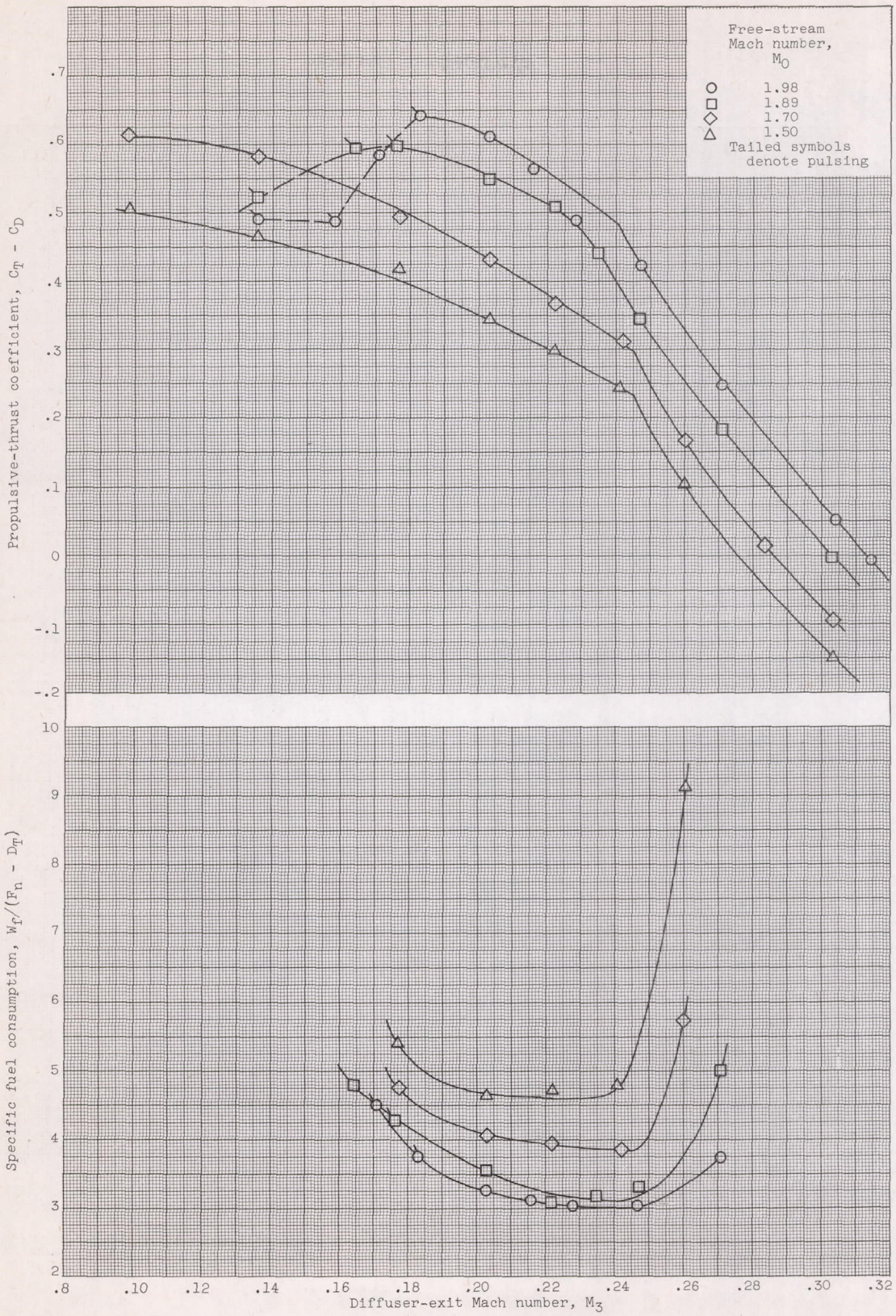

(b) Unshrouded inlet.

Figure 10. - Concluded. Propulsive thrust coefficient and specific fuel consumption.

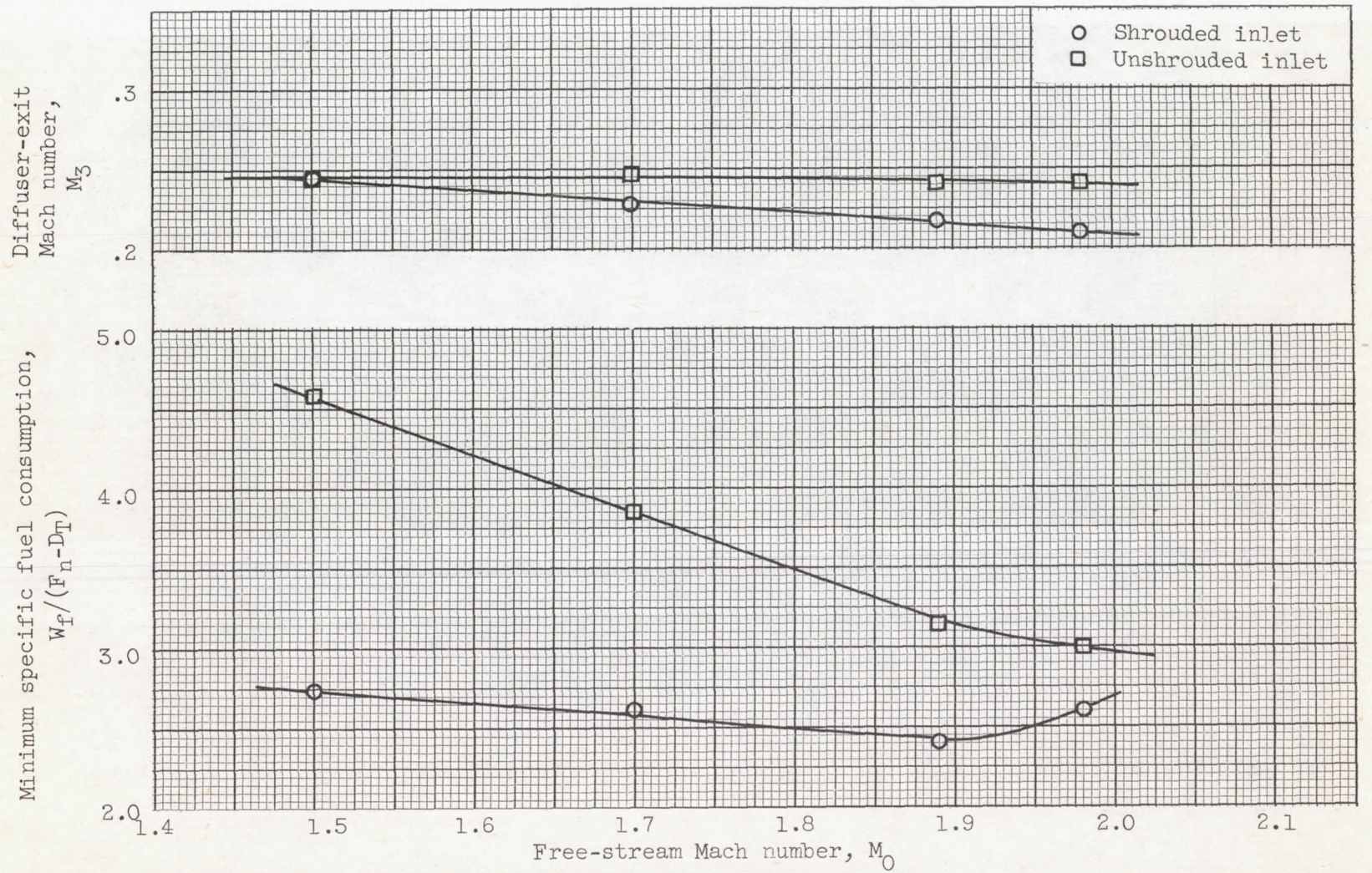

Figure 11. - Variation in minimum specific fuel consumption with free-stream Mach number for shrouded and unshrouded inlet configurations.

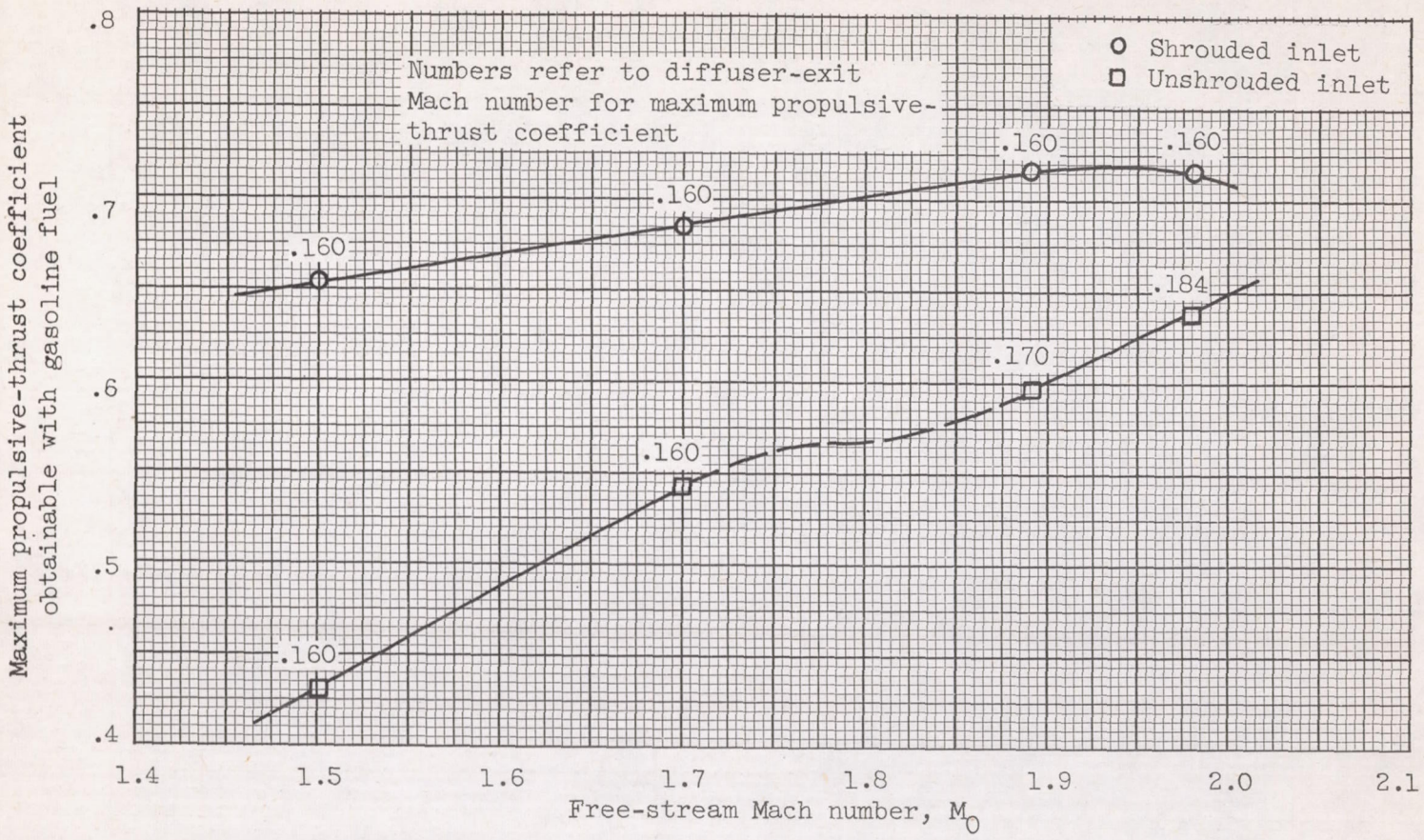

Figure 12. - Variation in maximum-propulsive thrust coefficient with free-stream Mach number for shrouded and unshrouded inlet configurations.